TBP at the Water−Oil Interface: The Effect of TBP Concentration and Water Acidity Investigated by Molecular Dynamics Simulations

M. Baaden,[†] M. Burgard,[‡] and G. Wipff*[,†]

Laboratoire MSM, Institut de Chimie, Université Louis Pasteur, UMR CNRS 7551, 4, rue B. Pascal, 67 000 Strasbourg France, and Laboratoire des Procédés de Séparation, ECPM, Université Louis Pasteur, UMR CNRS 7512, 25, rue Becquerel, F-67087 Strasbourg Cedex, France

Received: May 16, 2001; In Final Form: August 7, 2001

Molecular dynamics simulations provide microscopic pictures of the behavior of TBP (tri-*n*-butyl phosphate) at the water−"oil" interface, and in water−"oil" mixtures where "oil" is modeled by chloroform. It is shown that, depending on the TBP concentration and water acidity, TBP behaves as a surfactant, an interface modifier, or a solute in oil. At low concentrations, TBP is surface active and forms an unsaturated monolayer at the "planar" interface between the pure water and oil phases, adopting an "amphiphilic orientation". Increasing the TBP concentration induces water−oil mixing at the interface which becomes very rough while TBP orientations at the phase boundary are more random and TBP molecules solubilize in oil. The effect of water acidity is investigated with three nitric acid models: neutral NO_3H, ionic NO_3^- H_3O^+ and $TBPH^+$ NO_3^-. The role of these species on the properties of the water−oil boundaries and on the outcome of water−oil demixing experiments is presented. The neutral NO_3H form is highly surface active. Hydrogen bonding between TBP and NO_3H, $TBPH^+$, or H_3O^+ disrupts the first TBP layer and leads, at high TBP concentrations, to a mixed third phase or to a microemulsion. These results are important for our understanding of the microscopic solution state of liquid−liquid extraction systems.

I. Introduction

TBP (tri-*n*-butyl phosphate) is a particularly important molecule in the context of cation separation by liquid−liquid extraction.[1,2] Liquid TBP is completely miscible with organic solvents such as chloroform,[3] but nearly insoluble in water (x_{TBP} in water is 2.6×10^{-5} at 298 K[4]) as well as in acidic phases.[5,6] Since Warf discovered its extraction properties toward cerium,[7] TBP has become the cornerstone of the industrial PUREX ("Plutonium Uranium Refining by Extraction") extraction process to separate uranyl and plutonyl cations from nuclear waste solutions.[8−10] In this process, the metals are dissolved in a highly acidic aqueous source phase (about 3 M) and uranyl is extracted as $UO_2(NO_3)_2TBP_2$ complex by a mixture of organic solvents (TPH, kerosene with organic diluents) and TBP.[8] Another interesting aspect concerns its synergistic role in ion extraction. For instance, CYANEX-301 thiophosphoryl ligands extract Am^{3+} efficiently only in the presence of an excess of other phosphoryl-containing molecules such as TBP.[11,12] Another related facet concerns the amphiphilic character and surface activity of TBP which, at low concentrations (about 10^{-3} M) adsorbs at water−oil (dodecane or benzene) interfaces,[13−16] as do many related extractants and their complexes.[17,18] Beyond its important utilization, TBP serves also as a prototype for neutral organophosphorus or carbonyl-containing oxodonors used in complexation and liquid−liquid extraction of actinides and lanthanides. Indeed, very little is known about the microscopic behavior of such species in heterogeneous solvent environments, nor in synergistic extraction systems.

In this paper, we investigate the behavior of TBP in the presence of water and an immiscible liquid ("oil", modeled by chloroform), and the effect of water phase acidification. We use molecular dynamics (MD) simulations, based on a classical force-field representation of the potential energy. MD is a powerful tool to investigate liquid−liquid interfaces,[19] solvent mixtures,[20] as well as more complex assemblies such as micelles,[21] mono- or bilayers.[22] Our approach is to compare systems of increasing complexity simulated in consistent conditions. The first simulations considered TBP_n "oligomers" (*n* refers to the number of TBP molecules in the simulation box) at a preformed water−chloroform interface, where TBP_1, TBP_{10}, and TBP_{30} solutes were simulated starting from several initial positions.[23] It was shown that TBPs adsorb at a rather flat interface, pointing their phosphoryl dipoles toward the pH-neutral water and the alkyl chains in anhydrous "oil", but the interface was not saturated. Other simulations considered TBP as complexing or synergistic agent at water−chloroform[24] or water−supercritical-CO_2 [25] interfaces. The simulated concentrations were still lower than those used in synergistic systems or in the PUREX process (about 30% in weight). We thus decided to first model concentrated solutions, considering the pH-neutral TBP_{30} and TBP_{60} systems. The latter corresponds to about 30% of TBP, or 0.8 mol L^{-1}.

Inspired by the experimental conditions of cation extraction, we also investigate the effect of water acidity (about 1 M acid) on the properties of the water−oil−TBP systems, focusing on concentrated TBP_{30} or TBP_{60} systems. One important practical issue concerns the modeling of acidity. As in the classical force field methods we use, bond making and breaking processes cannot be modeled satisfactorily, an a priori choice has to be made concerning the status of the proton. Unfortunately, the latter is unclear from experiment for the simulated systems. In

* Author to whom correspondence should be addressed. E-mail: wipff@chimie.u-strasbg.fr.

[†] Laboratoire MSM, Institut de Chimie, Université Louis Pasteur.

[‡] Laboratoire des Procédés de Séparation, ECPM, Université Louis Pasteur.

10.1021/jp011890n CCC: $20.00
Published on Web 10/20/2001

pure water, reported pK_a values for nitric acid range from −1.44 to −3.78,[26] indicating that the 1 M acid is mostly dissociated. The TBP basicity is comparable to that of water. Its protonation has been investigated by ^{1}H and ^{31}P NMR[27] and IR spectroscopies.[28,29] For the benzene−TBP−aqueous nitric acid system, the surface tension γ displays peaks at HNO_3−TBP ratios of 1:1, 2:1, 3:1, and 4:1, but microscopic interpretations of these peaks are lacking.[14] The lack of precise experimental data on the proton state in nitric acid water−oil−TBP mixtures led us to consider hypothetical models of nitric acid, which likely contribute to the reality: one "neutral" (NO_3H) and one "ionic" (fully dissociated to NO_3^- H_3O^+). In an aqueous environment, the neutral model is less realistic than the ionic one, but more likely represents the acid extracted to an organic phase. The simulated TBP molecules are either all neutral or partially protonated as $TBPH^+$ species.

In addition to "standard" MD simulations at a preformed interface, we consider the demixing of water−oil−TBP mixtures. Demixing simulations with diluted solutions of salts,[30,31] of extractant molecules such as calixarenes[30] led to complete phase separation and adsorption of the extractants and of some ions at the formed liquid−liquid interface.[32,33] They are important to investigate the extent of separation of the water and oil phases and the distribution of TBPs after demixing. Do TBPs adsorb at the interface and is the interface fully covered? Do the more remote TBPs "randomly" dissolve in the organic phase, or form a second structured layer? Is there solvent mixing and is water "dragged" into the organic phase?

We wished we could consistently explore all different systems, with all combinations of variables, i.e., the three acidity models, the two TBP concentrations, with standard as well as with demixing MD simulations. This would require computer times beyond our present means. Therefore, selected combinations and models are presented in the following.

II. Simulation Methods

The MD simulations were performed with the AMBER5.0 software[34] where the potential energy U is described by a sum of bond, angle, and dihedral deformation energies, and pairwise additive 1−6−12 (electrostatic + van der Waals) interactions between nonbonded atoms.

$$U = \Sigma_{bonds} K_r (r - r_{eq})^2 + \Sigma_{angles} K_\theta(\theta - \theta_{eq})^2 + \Sigma_{dihedrals}\Sigma_n V_n(1 + \cos n\phi) + \Sigma_{i<j} [q_i q_j/R_{ij} - 2\epsilon_{ij}(R_{ij}^*/R_{ij})^6 + \epsilon_{ij}(R_{ij}^*/R_{ij})^{12}]$$

Parameters for the solutes were taken from the AMBER force field[35] and from previous studies in pure homogeneous solvents. The atomic charges of TBP are from ref 23 while those of $TBPH^+$, NO_3H, NO_3^-, and H_3O^+ were fitted from ESP ab initio calculations at the HF level using the 6-31G* basis set. They are given in Figure 1 with the corresponding AMBER atom types.

Water was represented with the TIP3P model[36] while we used the all atom model of Chang and Dang without polarization for chloroform.[37] Note that some simulations on TBP_{30} systems were previously reported with the OPLS united atom model of chloroform.[33,38] The nonbonded interactions were calculated with a twin residue based cutoff of 12/15 Å. All bonds were constrained with SHAKE, using a time step of 2 fs.

The interface has been built as indicated in ref 30 starting with two adjacent boxes of pure water and chloroform, respectively (Figures 2 and S1). The TBPs were initially placed

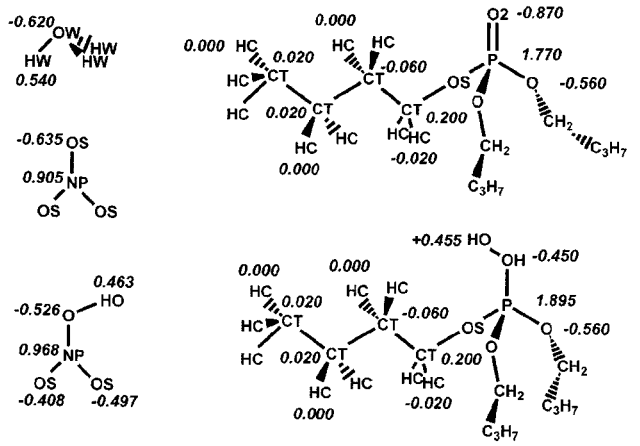

Figure 1. Schematic representation of TBP, $TBPH^+$, NO_3^-, and H_3O^+ with AMBER atom types and atomic charges.

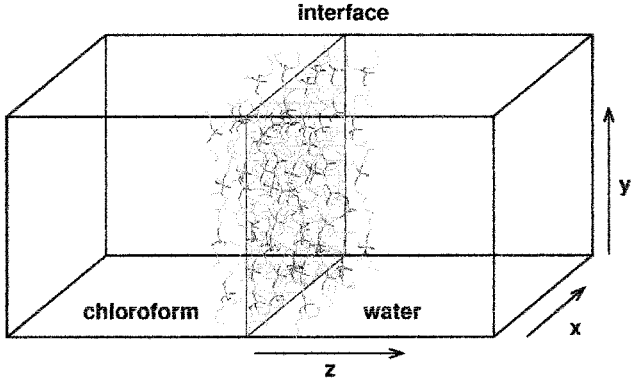

Figure 2. Schematic representation of the simulation box, with four layers of TBP (initial structure).

at the interface with 15 molecules per layer and the phosphoryl O_P oxygens pointing to water. The initial distribution of the other species is indicated below in the corresponding results sections and shown in Figure S1. In the standard simulations the systems were represented as in ref 39 with 2D periodic boundary conditions applied along the X and Y directions (see Figure 2), using an harmonic restraining potential at the Z-boundaries (with a force constant of 50 kcal mol^{-1} Å^{-2}). There are thus two solvent slabs, each of them being involved in a liquid−air and a liquid−liquid interface. For the mixing and demixing simulations the systems we applied 3D boundary conditions along the X, Y, and Z directions.

The simulation conditions and definitions of the different systems, further referred to as ***A*** to ***E***, are given in Table 1. After energy minimization and MD equilibration at a constant pressure of 1 atm, the dynamics was run at a constant volume and at 300 K, independently coupling the water subsystem and the remaining subsystem to a thermal bath, with a relaxation time of 0.1 ps. Standard MD was run for at least 1 ns, while demixing MD was run from 3 to 5 ns (Table 1).

Computer mixing experiments started at the end of the standard MD simulations by heating the system to 700 K, and scaling down the Coulombic interactions by a factor of 100. From the solvent and solute density curves, we checked that satisfactory mixing was achieved, after about 1 to 2 ns. Figure S2 illustrates the mixing of the very heterogeneous system ***E*** (45 TBP, 15 $TBPH^+$, 15 NO_3^-, 36 HNO_3, water, chloroform) during 1.5 ns. Demixing was performed by resetting the temperature to 300 K and the dielectric constant to 1.0.

The results were analyzed as described in ref 30 from the coordinates which were saved every 0.2 ps. The position of the

TABLE 1: Characteristics of Simulated Systems: Number of Solvent Atoms, Box Sizes, and Simulation Time [ns]

	system	$N_{Clf} + N_{wat}$	box [Å^3]	time[a] [ns]
A	30 TBP	406 + 1598	40 × 40*(39 + 34)	1.9
B	60 TBP	304 + 1323	37 × 36*88	2.0/1.0/4.5
B′	60 TBP (perpendicular)	304 + 1323	38 × 37*79	2.1
C	30 TBP−36 HNO_3	405 + 1794	40 × 40* (37 + 42)	2.0/2.0/5.1
D	30 TBP−36 H_3O^+−36 NO_3^-	405 + 1794	40 × 40 × (37 + 42)	1.0 2.1
E	15 $TBPH^+$−45 TBP/15 NO_3^-−36 HNO_3−36 H_2O	392 + 1628	36 × 36 × 103	1.7/1.5/3.0

[a] The times given are for equilibration/mixing/demixing, respectively

interface was recalculated as the intersection between the water and chloroform density curves. The distribution of different species was characterized by the corresponding density curves recentered at the interface and visual examination of the trajectories. The demixing index χ_{demix} has been defined as in ref 30 and ranges from 1.0 for a perfectly mixed water−oil systems to 0.0 for nonoverlapping separated phases.

The instantaneous water surface at the interface was determined by selecting the water molecules of minimal *Z* value (see Figure 2) which retain short contacts (O···O distances less than 4 Å) with at least two other water molecules, therefore excluding extracted or isolated water molecules.

III. Results

We first describe the pH-neutral water with TBP_{30} and TBP_{60} as solutes only. Then the effect of water acidity is modeled with a total of 30 or 60 TBPs. The systems are inherently dynamic and complex, and therefore difficult to describe in detail. They have been observed with care in stereo at the computer graphics system. In the following, we mostly display views obtained at the end of the simulations, and focus on statistical distributions of the solutes and solvents, characterized by density curves. In some cases, liquid phases are not well separated and the interface is therefore ill-defined, making such representations more difficult to interpret. The initial arrangements of systems ***A*** to ***E*** are shown in Figure S1 (Supporting Information).

1. The TBP Saturated pH-Neutral Water−Chloroform Interface with 30 and 60 TBP Molecules (systems *A* and *B*). TBP has significant influence on the shape and properties of the interface, as well as on the extent of water−oil separation. This is shown by the comparison of the TBP_{30} system ***A*** and the TBP_{60} system ***B***, from standard and demixing simulations.

1.1. Simulations at the Preformed Water−Chloroform Interface. The simulation of the TBP_{30} system ***A*** started with two unsaturated layers of 15 TBPs each. After 2 ns, the results were similar to those obtained by Beudaert et al. using another chloroform model.[38] During the simulation, only a few TBPs of the second layer diffused to the first layer which remained unsaturated (Figure 3). The TBPs oscillated between a few Ångströms up to 15 Å from the interface, indicating that the system was not trapped in a potential well and that the lack of saturation of the interface does not artifactually result from insufficient sampling. Finally, water is dragged to the organic phase, forming TBP hydrates, in line with NMR studies.[40−42] One observes TBP:H_2O supermolecules of 1:1, 1:2 and 2:2 stoichiometry near the interface (Figure 4). Such species have been inferred from Karl Fischer titrations of water−saturated chloroform.[42−44] The most important result is the irregular structure of the TBP layer at the interface, which is very different from the picture of a classical monolayer (Figure 5) and from the picture obtained with a less concentrated TBP_{10} system.[23] Also notice the migration of two TBPs to the bulk oil phase and the mixing of water and chloroform at the phase boundary. The phosphoryl groups of the TBPs next to the interface point toward the water phase as shown by the scatter plot of their P═O dipole μ_z in the z-direction (Figure 6). The interfacial μ_z value reaches up to almost −10 D, and in the second more remote layer, the orientation of the dipoles is reversed (+10 D). The corresponding angles with respect to the XY plane range from about 0° (tangential P═O orientation) to ±90° (perpendicular orientations).

The more concentrated TBP_{60} pH-neutral system was simulated with two initial configurations, where the four layers of 15 TBP are either parallel (***B***) or perpendicular (***B′***) to the interface. After equilibration, both yield similar distributions (Figure 3). The water−chloroform interface is severely perturbed by the presence of the TBP molecules, and is very "bumpy". One important difference, compared to the TBP_{30} system ***A***, is the increased mixing of chloroform and TBP (Figure 3). No distinct layers are observed any more. Instead, a mixed phase connects the bulk water and oil phase. On the average, about 0.7−1.1 waters per extracted TBP molecule are dragged to the organic phase forming TBP hydrates, as seen above with the TBP_{30} system. Compared to the TBP_{30} system, the proportion of $Cl_3CH\cdots O_{TBP}$ hydrogen bonds per TBP increases (from 0.2 to 0.8), while the proportion of $HOH\cdots O_{TBP}$ bonds decreases (from 1.3 to 0.9). On the other hand, TBP molecules do also enter the water layer and drag chloroform with them, two of them forming a dimer via hydrophobic association of their alkyl chains. Such mode of TBP dimerization in water is supported by experimental[42,45−47] as well as theoretical studies.[23]

Concerning the orientation of the P═O dipoles for the 60 TBPs, the μ_z scatter plot is less clear-cut than for the 30 TBP system (***B*** vs ***A***; Figure 6), but there is still a preferential amphiphilic orientation of the interfacial TBPs, hydrogen bonded to about 2 H_2O molecules.

1.2. Demixing Simulations on TBP_{30} and TBP_{60} pH-Neutral Systems. Demixing simulations with TBP_{30} as solute lead to rapid phase separation (less than 1 ns) and formation of two water−oil interfaces, onto which the TBP are spread, forming two unsaturated monolayers, where the O_P oxygens are hydrogen bonded with water (Figures 3 and S3). The water and oil phases are finally well separated, without mixing beyond the interfacial region. The organic phase is dry, while the aqueous phase contains no chloroform molecules. The final picture is nearly identical to the one obtained using the OPLS representation of chloroform[33] but somewhat differs from that obtained from the standard simulation ***A*** where TBP concentrated at one interface only.

A different case is observed with an increased concentration of 60 TBPs (Figures 3 and S4). First, phase separation is very slow. At 3 ns, two water "bubbles" are still immerged in a very mixed oil phase. A water slab forms later (at about 4 ns), adjacent to an oil phase which consists of a humid TBP−chloroform mixture. Finally, the water phase is quite homoge-

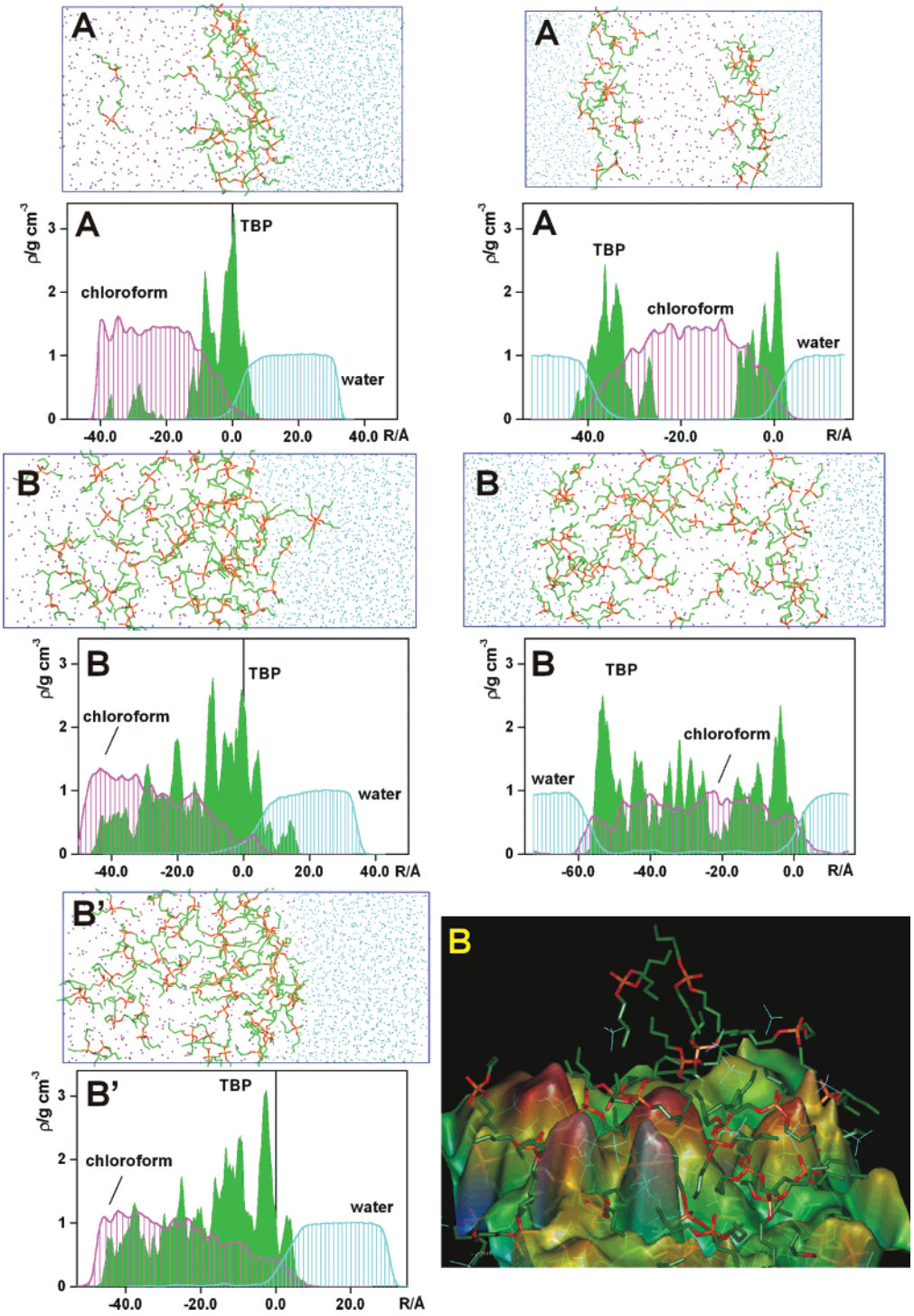

Figure 3. The pH-neutral TBP−water−choroform interfacial systems ***A*** (30 TBP), ***B*** (60 TBP, parallel to the interface), and ***B′*** (60 TBP, perpendicular to the interface) at the end of the standard simulation (left) and of the demixing simulation (right). For clarity the solvent molecules are shown as points. Density profiles (g/cm^3) of the solvents and TBP are shown for the last 100 ps. The TBP densities are given in arbitrary units. Bottom right: surface of water at the interface of system ***B*** (with chloroform on top; not shown).

neous and nearly pure (it contains a few chloroform molecules but no TBP), but does not form a clear-cut interface with oil. Even after a 4-fold increase of the demixing time, compared to the TBP_{30} system (4.6 ns), no discrete interface(s) have formed (Figure 3). The water surface is very irregular and more or less curved instead of being "flat" on the average. Surprisingly, the TBP molecules near this "interface" adopt more random orientations (see μ_z plots in Figure 6) and only a few of them form hydrogen bonds with interfacial water molecules. At the end of the dynamics, the mixed TBP−oil phase is very humid and contains about fifty water molecules. Some of them make hydrogen bonds with TBP molecules, others form local water networks or chains of up to eight water molecules isolated from the interface. As in the standard simulations ***B*** and ***B′***, the layer arrangement of TBPs is thus completely lost.

2. Acidic Biphasic Systems Containing TBP. Here, we consider the 30 TBP−36 HNO_3 acid system (***C***) and the corresponding fully ionic H_3O^+ NO_3^- one (***D***), as well as a partly protonated TBP−$TBPH^+$−NO_3^-−HNO_3 mixture (***E***). Comparison of these systems demonstrates the role of TBP and of the protonic state of nitric acid on the properties of the "interface" and on the microscopic nature of the solution.

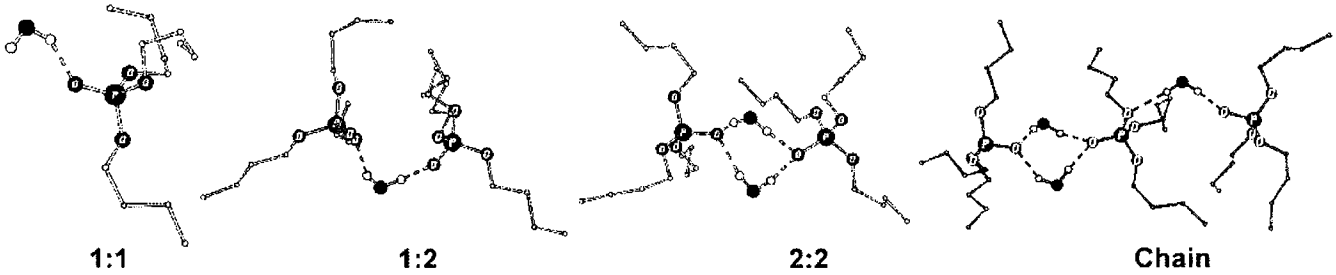

Figure 4. Typical TBP complexes formed with TBP and H_2O, observed at the end of simulation ***A***.

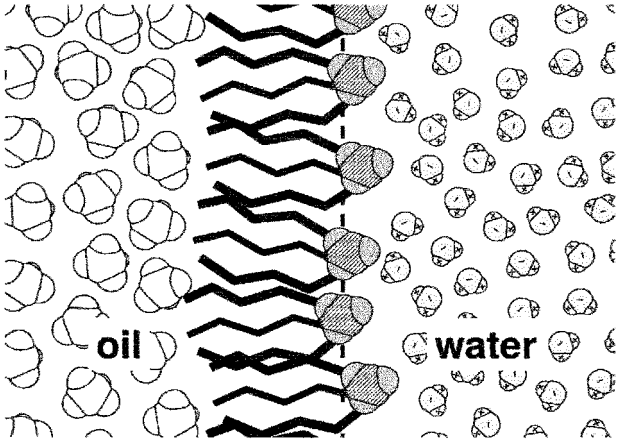

Figure 5. A schematic picture of a TBP monolayer as expected for classical surfactants.

*2.1. The TBP Saturated Acidic Interface: Neutral NO_3H Model (system **C**).* Standard simulation ***C*** started with 36 HNO_3 molecules diluted in the bulk aqueous phase, without contact with the interface, and a model-built bilayer of 2 × 15 TBPs positioned at the interface. Very rapidly the majority of the HNO_3 molecules migrated to the disordered interfacial TBP layer, forming 1:1 and 2:1 complexes with TBP (Figures 7 and 8). In the literature mainly 1:1 complexes were discussed,[43,48] but a few authors report complexes up to 4:1 stoichiometry.[49,50] In our simulations several HNO_3:TBP complexes were completely extracted to the organic phase, which is also consistent with the extraction of nitric acid by TBP as reported in the literature.[51,52] Some TBPs became "complexed" with water, as in the pH-neutral systems. The distribution of the HNO_3 species was characterized by the corresponding density curves (Figure 7). After the first nanosecond, about 60% of these species were found within 7 Å from the interface, while 40% remained in water, close to the interface. After 2 ns, only 20% of the acid is in bulk water, the majority being concentrated on the water side of the interfacial TBP layer, while another fraction has been extracted to chloroform by TBP molecules (see the density curve of Figure 7). An interesting phenomenon was the formation of a water "pocket" on the organic side of the interface, consisting of about 10 water molecules surrounded by several TBPs and HNO_3 molecules (Figure 8). This pocket remained in chloroform until the end of the simulation, at about 15 Å from the interface, without hydrogen bond connections with the interfacial water.

At the interface, a first layer of about 20 TBPs, up to 10 Å thick, is in contact with the aqueous phase. It is not compact enough, however, to fully cover the water surface and only few P═O dipoles point to the aqueous phase, due to the preferred hydrogen bonds with interfacial HNO_3 molecules. The remaining TBPs spread into the organic phase, where they are almost randomly dispersed and penetrate up to a distance of about 20 Å from the interface. Most of them are hydrogen bonded to co-extracted HNO_3. One also notices that the second "layer" of TBPs is less well defined than in the acid-free TBP interface (compare density profiles in Figures 3 and 7 and μ_z plots in Figure 6).

Comparison with simulation results on the neat acidic water−chloroform interfaces[53,54] reveals the importance of TBP on the acid distribution. Without TBP, HNO_3 molecules also accumulate at the interface, but are absent in the oil phase, while the added TBP drags the HNO_3 species to the oil phase. In both systems, interfacial HNO_3 molecules are hydrogen bonded to water molecules via their NO−H proton.

The main features obtained by the standard MD simulations are confirmed by the demixing simulation of system ***C*** (Figures 7 and S5). A complete phase separation is observed on the nanosecond time scale and, in contrast to the equilibrated "standard" system ***C***, *all* HNO_3 molecules are trapped at one of the two interfaces. About half of the TBP and half of the acid molecules sit at each formed interface. The picture emerging from this long simulation (5.2 ns) is a dynamic one: some acid molecules migrate from one interface to the other, crossing the organic layer "transported" as TBP:HNO_3 complexes. Occasionally, one to a maximum of five HNO_3 molecules move to the water phase but return to one of the interfaces thereafter. This somewhat contrasts with the results of the standard simulation where the fraction of HNO_3 molecules in water was larger, likely because the interface was more "saturated" by TBP and HNO_3 species. Hydrogen bonded chainlike or stacked arrangements of NO_3H molecules are frequently observed, but their lifetime is short (about 10 ps).

*2.2 The TBP Saturated Acidic Interface: Ionic NO_3^- H_3O^+ Model (system **D**).* The simulation ***D*** started with a grid of 36 H_3O^+ NO_3^- ions in the aqueous phase, a regular 2 × 15 TBP bilayer right at the interface, and a pure organic phase.[55] At the end of the dynamics the water and organic phases remain separated by a very irregular "interface" (Figure 7). The bulk organic phase is free of any ionic species, but solubilizes TBP hydrates. Several dynamically changing water "protuberances" are observed on the organic side of the interface. The phase boundary is loaded with some acid and water. The hydrophilic H_3O^+ and NO_3^- species prefer the aqueous phase. However, a noticeable proportion of H_3O^+ cations sit at the interface (Figure 7), hydrogen bonded with TBPs.

The TBP molecules at the interface form a bulky, curved arrangement which differs from the pH-neutral system ***A*** where a more layerlike structure was observed. The TBP positions and orientations in ***D*** are also more randomized than in ***A*** (Figure 6). Surprisingly, few TBPs only adopt amphiphilic orientations. Along the dynamics, they move somewhat to the water side of the interface, where eight of them sit at the end of the simulation. The driving force seems to be the formation of TBP:H_3O^+ "complexes" of 1:1, 2:1, and 3:1 type, some of them involving the NO_3^- counterions (Figure 9). These complexes are addition-

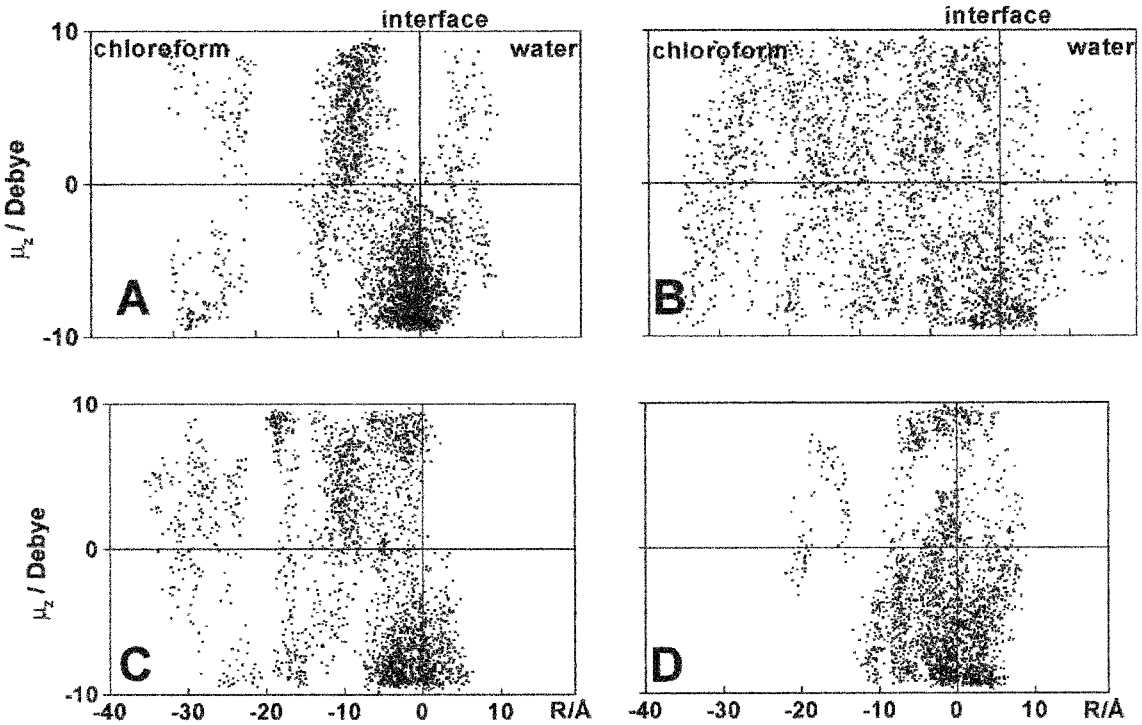

Figure 6. Scatter plot of the μ_z component of the TBP dipole moment as a function of z, accumulated over the last 500 sets of the "standard" dynamics of systems ***A***−***D***.

ally solvated by water molecules. Experimental studies by IR spectroscopy in acidic TBP solutions are in line with these findings and show the stepwise formation of proton hydrates H^+_n $(H_2O)_p$TBP with various possible stoichiometries.[28] Comparison of the neutral HNO_3 vs ionic NO_3^- H_3O^+ models of the acid reveals that the ions are more concentrated in water than neutral HNO_3, as expected. Thus, there are less TBPs interacting with H_3O^+ (35−45% in ***D***) than with HNO_3 (55% in ***C***), but more hydrogen bonds (76%) are formed per TBP due to the increased number of potential H-donor sites (up to three per H_3O^+ ion).

It is interesting to compare system ***D*** with the neat acidic water−chloroform sytem.[53] In the absence of TBP, the 36 H_3O^+ NO_3^- ions are "repelled" by the neat interface and solubilized in bulk water.[53] The resulting phase boundary between water and oil is well defined and relatively flat. When TBP is added to the system, it concentrates at the interface where it attracts H_3O^+ and NO_3^- ions. This induces more solvent mixing at the interface which becomes less well defined and facilitates the possible protonation of TBP (vide infra).

*2.3. Protonation of TBP in an Acidic System Containing Nitric Acid (system **E**).* TBP protonation has been addressed by simulation of system ***E*** starting with three neutral layers of 3 × 15 TBPs, next to one protonated layer of 15 $TBPH^+$ in contact with an acidic water phase containing 15 neutralizing NO_3^- counterions and 36 HNO_3 molecules. The snapshots and density profiles given in Figure 7 reveal new important features. The TBPs retain more or less a three-layer structure but, interestingly, some TBP and $TBPH^+$ molecules exchanged between the first two layers, as a result of $TBPH^+$−$TBPH^+$ intralayer repulsions, of counterion effects, and of specific TBP···$TBPH^+$ attractions. Visual inspection of the trajectories reveals the frequent formation of 1:1 and 1:2 $TBPH^+$:TBP adducts. As a consequence, the corresponding phosphoryl dipoles do not point toward water, in contrast to expectations for diluted solutions of TBP or $TBPH^+$ amphiphilic species. At the end of the simulation ***E***, the first TBP layer on the water side is half protonated/half neutral, without being, however, saturated. The second layer is slightly protonated and in majority neutral, and a third fraction immersed in chloroform is neutral. The protonated $TBPH^+$ species are partly neutralized (up to 60%) by two associated "layers" of nitrate counterions, whereas 40% of the remaining anions sit in the bulk aqueous phase (at more than 15 Å from the interface). Surprisingly, no nitric acid is extracted to the organic phase, presumably because of the screening effect of TBPs at the interface. The majority of the HNO_3 molecules are either in water or at the interface. Compared to the pH-neutral systems ***B*** and ***B′*** comprising the same number of 60 TBP molecules, the interfacial TBP layer is more compact and confined when $TBPH^+$ is present, indicating an enhanced surface activity of the protonated species. The interfacial "layer" contains substantial amounts of water, and the system as a whole can be seen as a three-phase entity, which is a "third phase"[56−59] consisting of a humid TBP−acid−oil mixture.

Third phase formation is supported by the demixing simulation of system ***E*** (Figure 7) which leads to a somewhat different picture than the "standard" simulation. Upon demixing, system ***E*** also differs from system ***B*** which contains the same number of TBP molecules, but no nitric acid. At the end of the dynamics (3.1 ns) no complete phase separation has taken place. The water and chloroform phases no longer form slabs, but a kind of microemulsion where water or chloroform "bubbles" dynamically exchange with mixed solvent environments. At the end of the simulation one perceives (Figure 7) three types of microsolvent structures: one neat water bubble containing nitrates, one pure chloroform bubble, and one rather mixed humid TBP−HNO_3−chloroform microphase. The TBPs are spread in an interfacial network all over the simulation box, held by hydrogen bonded $TBPH^+$ and HNO_3 species. Other TBPs sit in unstructured mixed organic microphases. The difference between acid (***E***) and neutral acid-free TBP_{60} (***B***) systems clearly hints at the impact of protonated and ionic species on the solution state of the mixture and on the nature of the water−oil interface.

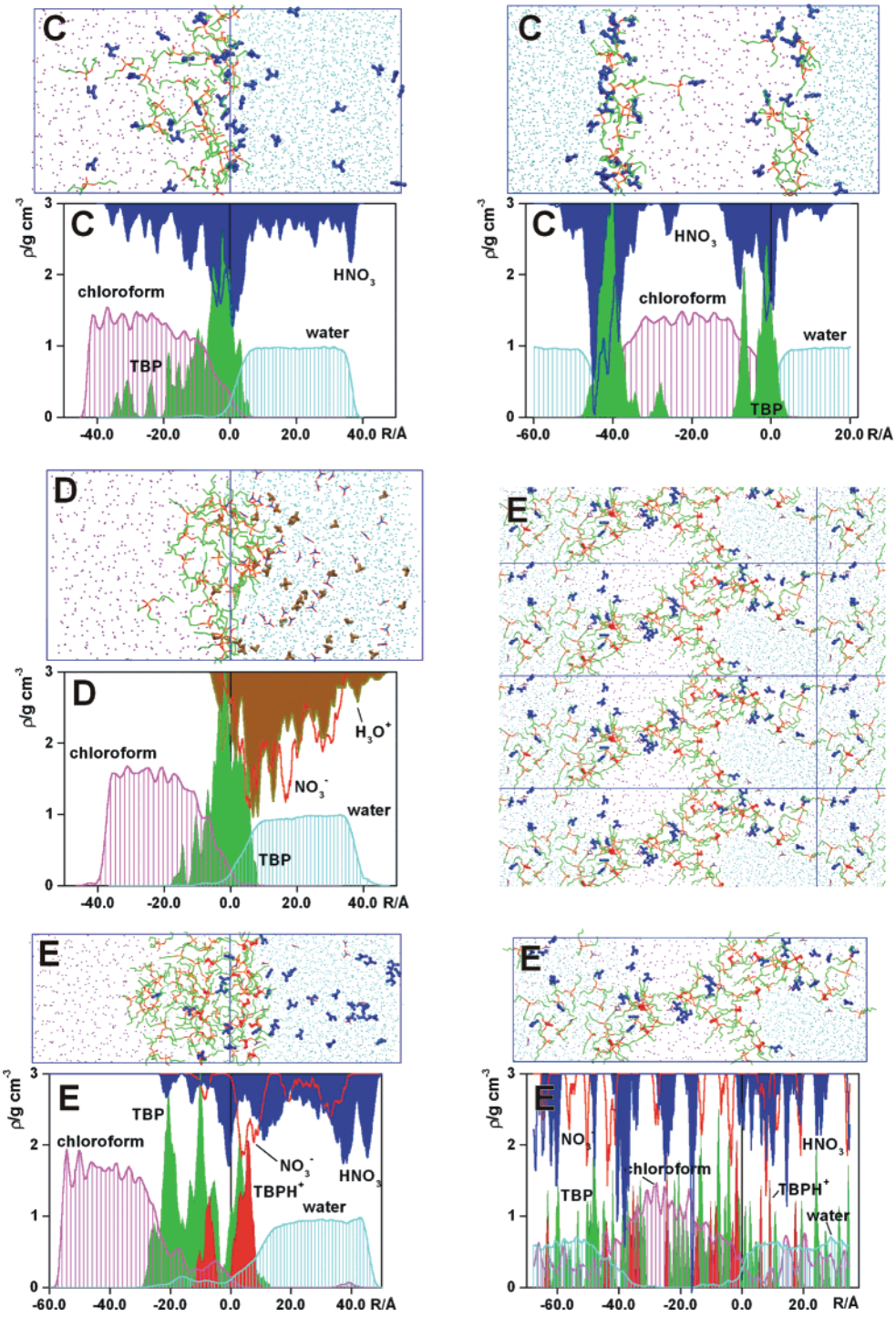

Figure 7. The acidic TBP−water−choroform interfacial systems ***C*** (30 TBP−36 HNO_3), ***D*** (30 TBP−36 H_3O^+ NO_3^-), and ***E*** (45 TBP−15 $TBPH^+$−36 HNO_3−15 NO_3^-) at the end of the standard simulation (left) and of the demixing simulation (right). For the final view of demixing ***E***, the simulation box is also repeated with 2D translations. For clarity the solvent molecules are shown as points. Density profiles (g/cm^3) of the solvents and TBP are calculated during the last 100 ps. The solute densities are given in arbitrary units and shown "up side down" units for clarity.

IV. Discussion and Conclusion

MD simulations on several models of interfacial systems involving nitric acid and TBP reveal the effect of acid representation (ionic vs neutral), TBP protonation and concentration. Generally, "standard" MD simulations starting with a preformed interface yield the same trends as the demixing simulations at low concentrations of the solutes. The major difference originates from the fact that in demixing simulations, the surface active solutes tend to dilute onto the two forming liquid−liquid interfaces, instead of concentrating at one of them. Only in the case of the heterogeneous acidic complex system ***E*** does demixing not lead to phase separation, but to formation of a microemulsion of "solvent bubbles" in a TBP−oil mixture.

The demixing simulations demonstrate that at neutral pH and at low TBP concentrations, the "perfectly mixed" water−organic mixtures separate rapidly, on a nanosecond time scale, indicating that the water−organic liquids are never completely mixed at the microscopic level, but separated by an interface. As the TBP concentration is increased and nitric acid is added, the interfacial TBPs loose their layer structure and form a disordered medium

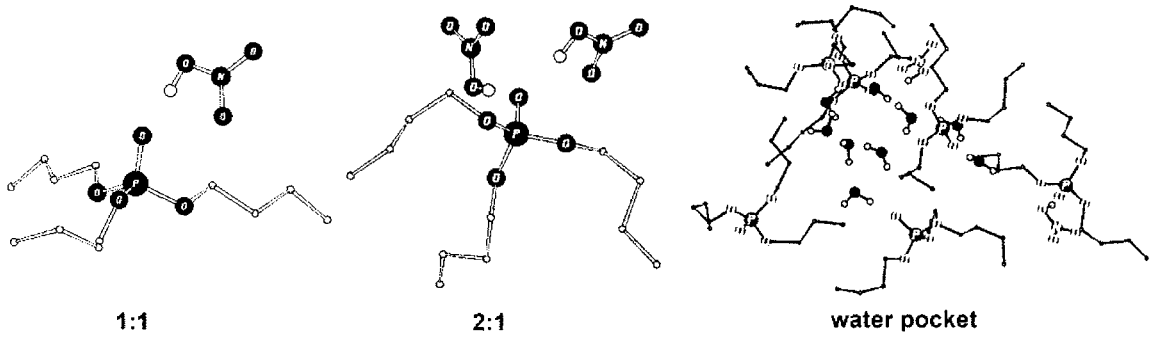

Figure 8. Typical complexes of TBP and HNO_3, and the "water pocket" (concentrated TBP hydrates) which formed in bulk chloroform at the end of standard simulation ***C*** (30 TBP, 36 NO_3H).

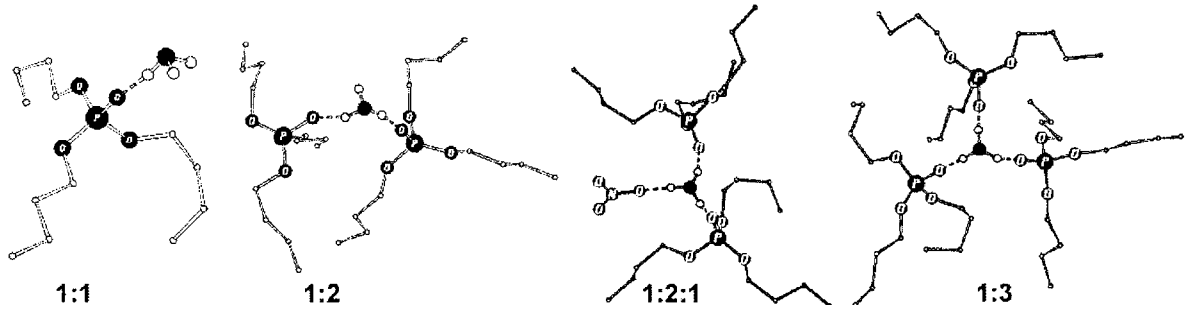

Figure 9. Typical complexes of TBP with H_3O^+ (1:1, 1:2, 1:3) and with $H_3O^+ NO_3^-$ (1:2:1) at the end of simulation ***C*** (30 TBP, 36 $NO_3^- H_3O^+$).

("third phase") between the oil phase and the aqueous phase, or a microemulsion. We notice that in real demixing experiments, the macroscopic phase separation is furthermore driven by gravitational or centrifugational forces. This leads to a collapse of microdroplets and decrease of the interfacial area, likely accompanied by desorption of the third phase from the interface and its extraction to the organic phase. These events involve time scales and dimensions which are presently not amenable to MD computational approaches.

What is the "Interface"? How Do Concentrated Solutions of Surface Active Species Behave? Throughout the paper, we refer to the water−oil interface for simplicity, but this region is in some cases ill-defined and its characteristics evolve with the TBP and acid concentration. As can be seen from the snapshots of Figures 3 and 7, the surface and density of water are better defined than the surface and density of oil, especially when TBP or nitric acid molecules concentrate at the interface. As a result, the Z-position of the interface, calculated from the intersection of the two solvent density curves, may undergo large fluctuations and uncertainties as a function of time. In addition, the interface is never planar, as illustrated by the instantaneous water surface of system ***B*** (Figure 3). This surface is very rough and displays troughs and mounds. It is also inherently dynamic, as troughs and mounds exchange in periods ranging from about fifty to a few hundreds picoseconds. There are no straightforward indices to characterize time-dependent shape, roughness, and thickness of the surface. Examination of water surface at the graphics system clearly reveals increasing loss of average planarity and enhanced rugosity when the acid or TBP concentrations are increased. One extreme case would be the surface of water micropools found in the demixing of system ***E*** (Figure 7). What would happen with a larger simulation box remains to be investigated. This is why the "interface", local boundary region of water and oil, may in fact range from solvent microheterogeneities (e.g., formed upon strong agitation of the extraction system) to the surface of microdroplets or to parts of a macroscopic interface at rest.

One of the motivations of this study was to investigate the possible saturation of the interface by TBP and to characterize its resulting orientations. We find that the interface is in no case fully covered by a TBP monolayer, likely because the alkyl chains are too short and TBP is of "conic shape", leading to disordered arrangements at the interface. In our simulations disorder gradually increases from the neat interface (no acid), to the neutral and ionic acid interfaces. This loss of interfacial structure with ionic acid models may be viewed as a first step toward the formation of mixed solutions involving associates, as suggested by experiment.[59−61] Interestingly, it has been found that near the critical temperature a third phase often forms at water−liquid interfaces, and that the this phenomenon is enhanced by added salts.[62] This is consistent with the trends observed in our simulated ionic systems.

Interfacial Distribution of Nitric Acid. In our simulations, the acid is either neutral HNO_3 or dissociated to NO_3^- and H_3O^+. In the absence of TBP, the ionic species are "repelled" by the interface, while the neutral HNO_3 molecules are surface active.[53] A recent spectroscopic study of aqueous nitric acid solutions at the water−air surface, which bears analogies with the water−oil interface, corroborates these findings.[63,64] In the presence of TBP a peak of nitric acid concentration is also observed at the interface for the neutral HNO_3 form and, to a lesser extent, for the ionic forms, which both display specific hydrogen interactions with TBP. Thus TBP promotes acid concentration in the interfacial region.

TBP also promotes the extraction of the acid to the organic phase. While in simulations without TBP, no nitric acid extraction was observed,[53] we find that nitric acid is extracted as HNO_3:TBP adducts of 1:1 and 2:1 types. Simulations with the ionic model lead to H_3O^+:TBP adducts of 1:1, 1:2 and 1:3 types and significant mixing of the chloroform, TBP, and water

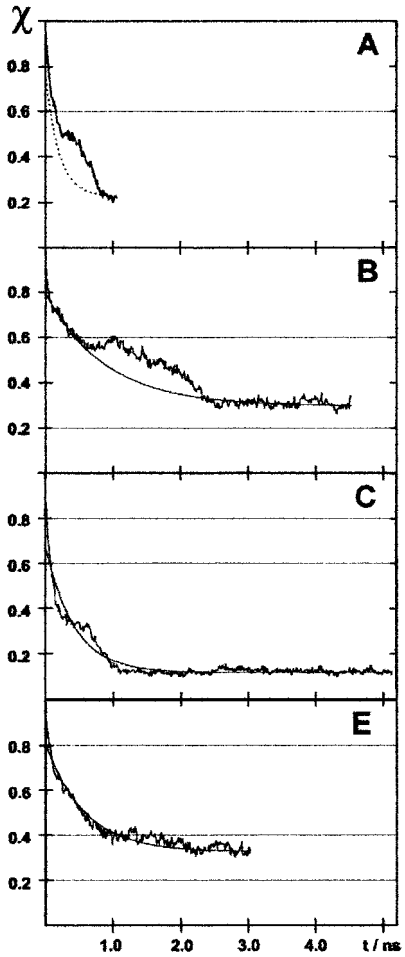

Figure 10. Demixing simulations ***A*** to ***E***: demixing index χ_{demix} as a function of time.

liquids in the interfacial region, but no acid extraction, indicating that the acid is extracted in its neutral HNO_3 form or, to a lesser extent, in the ionic $TBPH^+$ NO_3^- form. Interestingly, the high degree of association of $TBPH^+$ with neutral TBPs, H_2O, or NO_3^- species near the interface found in simulation ***E*** is consistent with the formation of TBP aggregates of 4−5 TBP molecules in the oil phase at high nitric acid concentration, recently characterized by X-ray and neutron diffraction experiments.[65]

Demixing of Mixed Water−Oil Solutions. The difficulty to prepare homogeneous mixed solutions starting from the two adjacent liquid phases (more than one nanosecond simulation at high temperature using biased potentials were needed) shows the reluctance of water and oil to mix. Conversely, phase separation from mixed systems is initiated quite readily, generally starting with self-aggregation of water. What happens next depends on the system. At low TBP concentration (TBP_{30} system ***A***), the water and oil phases separate totally in less than 1 ns, while in the more concentrated (TBP_{60}) or acidic systems, water forms either a single "vertical slab" (system ***B***) or microdroplets (water-in-oil microemulsion in ***E***). To characterize the kinetics of solvent separation, we calculated a demixing index χ_{demix} for each saved set of coordinates. This index, defined in ref 30, may range from 1 (for perfectly mixed phases) systems to 0 (for non overlapping separated phases). The time dependence for systems ***A*** to ***E*** is plotted in Figure 10. At 0 ps, χ_{demix} is about 0.75 for all systems, and drops to less than 0.2 in 1 ns for ***A*** and ***C*** where two "vertical" solvent slabs formed. This contrasts with the more concentrated and heterogeneous solutions ***B*** and ***E***, where a plateau is reached later (about 3 ns) and indicates that the phases do not separate further during the last nanosecond. The corresponding χ_{demix} value is still quite large (about 0.3), supporting the lack of spontaneous well-defined phase separation in these systems.

Implications Concerning the Mechanism of Assisted Ion Extraction. Our results have important consequences concerning the mechanism of assisted ion extraction, especially with highly charged cations such as actinides or lanthanides. The quasi-insolubility of neutral extractant molecules in water and of the hard cations in oil prevents their complexation in any of these phases. The fact that extractant molecules and their complexes are surface active rather suggests an "interfacial" extraction mechanism, provided that the ions can by sufficiently close to the "interface" to be complexed. At neutral pH and low extractant concentrations, the interface is locally well defined and "flat", and "repels" highly charged cations which are therefore hardly extractable.[31] Increasing the extractant concentration, as well as the acidity of the medium disrupts the interfacial water surface, and leads to a local mixed phase or solvent heterogeneities where complexation is facilitated. Such ion capture mechanism has been observed computationally in the case of uranyl cation extraction by TBP.[24,66] We suggest that there is some continuity between the local deformations of the interface (e.g., at the surface of droplets whose surface tension decreased) and the appearance of microemulsions and solvent microheterogeneities as found after the demixing simulation ***E***.

Coming to the lack of an interfacial TBP monolayer at high concentrations, we notice that this is a favorable feature for ion extraction. A saturated monolayer would display a shielding effect and prevent migration of the complex to the oil phase (see the analogy with the lack of acid extraction in the standard simulation of system ***E***). Instead, more "random" orientations of extractant molecules at an unsaturated interface facilitate the ion capture and extraction. We also notice that for example CMPO extractant molecules, which extract lanthanide cations, are inherently asymmetrical and likely do not form a saturated interfacial layer, thus promoting solvent mixing in the interfacial region. Phosphoryl-containing calixarenes, also surface active and good extractants for M^{3+} ions, may adopt multiple orientations at the phase boundary and promote solvent mixing.[67] A recent report of lanthanide extraction by water-in-oil microemulsions is in line with such effects.[68] It is stressed that formation of solvent heterogeneities or microemulsions is an important aspect of synergism, for instance in the CYANEX-301 extraction of M^{3+} cations where addition of about 30% TBP leads to enhanced extraction.[11]

Computational Issues. Finally, we would like to comment on computational aspects of this work. There are a number of issues concerning the modeling of acidity, the energy representation of the system, and size effects. Modeling of the acidity is a difficult task, especially in heterogeneous environments. The best models should allow for proton transfer between H_2O, TBP, NO_3^- molecules or aggregates and require quantum mechanical methods,[69,70] as reported for the nitric acid trihydrate.[71] We used a simpler force field approach, based on selected representations of neutral and dissociated acid. Other combinations and relative concentrations of these species could be tested, leading to more complex pictures.[72]

Concerning the MD simulations, we feel that there is no major artifact in the simulated results. Although the solvent parameters fitted for pure liquids may inaccurately describe their mutual interactions, we showed that several models of chloroform, some

of them including explicit polarization terms, lead to similar results in demixing simulations.[73] Inclusion of a polarization term in the force field does not significantly modify the properties of the interface.[74] The representation of the system boundaries (2D vs 3D) has also little effect on the interfacial properties.[73] The treatment of long range forces and electrostatic effects is another matter of concern, but difficult to solve in asymmetrical solvent environments. 2D-Ewald summation techniques are not presently available in Amber and may introduce other artifacts.[75,76] We tested standard vs reaction field corrected treatment of Coulombic interactions on related interfacial systems and obtained similar density profiles. Another issue concerns the sampling of the systems, in relation with the simulated times. In the case of calixarene solutes whose relaxation times are larger than for TBP, we found that the interfacial behavior obtained from MD simulations at preformed interfaces was the same as the one obtained from severely perturbed systems in which the two solvents were completely mixed.[30] As the times simulated here are at least twice as large as the time needed for liquid−liquid-phase separation (less than one nanosecond), the systems can be considered as equilibrated. What would happen at larger time scales and at larger size scales remains to be investigated in conjunction with larger cutoff distances and requires computer means beyond our present resources. Concerning the evolution from more or less deformed interfaces to microemulsions, another parameter to be investigated is the relative water−oil content. Our simulations started with similar volumes of both liquids, but other compositions should be studied.

We hope that such "computer experiments" will stimulate further theoretical and experimental studies on interfacial phenomena and solution properties of extraction systems. Beyond ion separation, the results bear impact on other fields such as interfacial electrochemistry,[77,78] phase transfer catalysis,[79] drug transport and availability at water phase boundaries near membranes, micelles, or polymeric surfaces.[80,81]

Acknowledgment. The authors are grateful to CNRS-IDRIS and to Université Louis Pasteur for allocation of computer resources. G.W. thanks the EEC (F1KW-CT2000-0088 contract), PRACTIS and COST D9 for support and Prof. C. Madic for stimulating discussions. M.B. thanks the French Ministery of Research for a grant.

Supporting Information Available: Six tables that include initial structures of the simulated systems ***A***−***E***; density curves in the z-direction for system ***E***; and demixing of systems ***A***, ***B***, ***C***, and ***E*** as a function of time. This material is available free of charge via the Internet at http://pubs.acs.org.

References and Notes

(1) Marcus, Y.; Kertes, A. S. *Ion Exchange and Solvent Extraction of Metal Complexes*; Wiley-Interscience: New York, 1969.

(2) Tedder, D. W. In *Science and Technology of Tributyl Phosphate*; Schultz, W. W., Navratil, Z. D., Kertes, A. S., Eds.; CRC Press, Boca Raton, FL, 1991; pp 35−70.

(3) Kharchenko, S. K.; Mikhailov, V. A.; Afanasiev, Y. A.; Ponomareva, L. I. *Akad. Nauk USSR, Izv. Sibirsk. Otd, Akad. Nauk SSSR, Ser. Khim. Nauk.* **1964**, *Chem. Abstr. 63, 12384a,* 30−37.

(4) Marcus, Y. *The Properties of Solvents*; John Wiley & Sons: Chichester, 1998.

(5) Kuno, Y.; Hina, T.; Masui, J. *J. Nucl. Sci. Technol.* **1993**, *30*, 567.

(6) Higgins, C. E.; Baldwin, W. H.; Soldano, B. A. *J. Phys. Chem.* **1959**, *63*, 118.

(7) Warf, J. C. *J. Am. Chem. Soc.* **1949**, *71*, 3257.

(8) Horwitz, E. P.; Kalina, D. G.; Diamond, H.; Vandegrift, G. F.; Schultz, W. W. *Solvent Extract. Ion Exch.* **1985**, *3*, 75−109.

(9) Cecille, L.; Casarci, M.; Pietrelli, L. *New Separation Chemistry Techniques for Radioctive Waste and Other Specific Applications*; Commission of the European Communities Ed.; Elsevier Applied Science: London, New York, 1991.

(10) Choppin, G. R.; Nash, K. L. *Radiochim. Acta* **1995**, *70/71*, 225−236.

(11) Modolo, G.; Odoj, R. *Solvent Extract. Ion Exch.* **1999**, *17*, 33−53.

(12) Ionova, G.; Ionov, S.; Rabbe, C.; Hill, C.; Madic, C.; Guillaumont, R.; Modolo, G.; Krupa, J.-C. *New J. Chem.* **2001**, *25*, 491−501.

(13) Tomoaia, M.; Andrei, Z.; Chifu, E. *Rev. Roum. Chim.* **1973**, *18*, 1547.

(14) Chifu, E.; Andrei, Z.; Tomoaia, M. *Anal. Chim. (Rome)* **1974**, *64*, 869−871.

(15) Sagert, N. H.; Lee, W.; Quinn, M. J. *Can. J. Chem.* **1979**, *57*, 1218.

(16) Haslam, S.; Croucher, S. G.; Hickman, C. G.; Frey, J. G. *Phys. Chem. Chem. Phys.* **2000**, *2*, 3235−3245.

(17) Szymanowski, J. *Solvent Extr. Ion Exch.* **2000**, *18*, 729−751.

(18) Watarai, H. *Trends Anal. Chem.* **1993**, *12*, 313−318.

(19) Benjamin, I. *Annu. Rev. Phys. Chem.* **1997**, *48*, 407−451 and references therein.

(20) Tarek, M.; Klein, M. L. *J. Phys. Chem. A* **1997**, *101*, 8639−8642.

(21) Smit, B.; Hilbers, P. A. J.; Esselink, K. *Tenside Surf. Det. 30* **1993**, *4*, 287−294.

(22) Tieleman, D. P.; Marrink, S. J.; Berendsen, H. J. C. *Biochim. Biophys. Acta* **1997**, *1331*, 235−270.

(23) Beudaert, P.; Lamare, V.; Dozol, J.-F.; Troxler, L.; Wipff, G. *Solvent Extr. Ion Exch.* **1998**, *16*, 597−618.

(24) Baaden, M.; Berny, F.; Muzet, N.; Troxler, L.; Wipff, G. In *Calixarenes for Separation. ACS Symposium Series 757*; Lumetta, G., Rogers, R., Gopolan, A., Ed.; ACS, Washington, DC, 2000, pp 71−85.

(25) Schurhammer, R.; Berny, F.; Wipff, G. *Phys. Chem. Chem. Phys.* **2001**, *3*, 647−656.

(26) Petkovic, D. M. *J. Chem. Soc., Dalton Trans.* **1982**, 2425−2427.

(27) Du, Y.; Peng, H.; Yuan, H.; Chen, L. *Acta Chim. Sinica* **1987**, *45*, 279−282.

(28) Stoyanov, E. S. *J. Chem. Soc., Faraday Trans.* **1997**, *93*, 4165−4175.

(29) Stoyanov, E. S. *Phys. Chem. Chem. Phys.* **1999**, *1*, 2961−2966.

(30) Muzet, N.; Engler, E.; Wipff, G. *J. Phys. Chem. B* **1998**, *102*, 10772−10788.

(31) Berny, F.; Schurhammer, R.; Wipff, G. *Inorg. Chim. Acta; Special Issue* **2000**, *300−302*, 384−394.

(32) Berny, F.; Muzet, N.; Schurhammer, R.; Troxler, L.; Wipff, G. In *Current Challenges in Supramolecular Assemblies, NATO ARW Athens*; Tsoucaris, G., Ed.; Kluwer Academic Publishers: Dordrecht, 1998; pp 221−248.

(33) Berny, F.; Muzet, N.; Troxler, L.; Wipff, G. In *Supramolecular Science: where it is and where it is going*; Ungaro, R., Dalcanale, E., Eds.; Kluwer Academic Publishers: Dordrecht, 1999; pp 95−125 and references therein.

(34) Case, D. A.; Pearlman, D. A.; Caldwell, J. C.; Cheatham, T. E., III; Ross, W. S.; Simmerling, C. L.; Darden, T. A.; Merz, K. M.; Stanton, R. V.; Cheng, A. L.; Vincent, J. J.; Crowley, M.; Ferguson, D. M.; Radmer, R. J.; Seibel, G. L.; Singh, U. C.; Weiner, P. K.; Kollman, P. A. *AMBER5*; University of California, San Francisco, 1997.

(35) Cornell, W. D.; Cieplak, P.; Bayly, C. I.; Gould, I. R.; Merz, K. M.; Ferguson, D. M.; Spellmeyer, D. C.; Fox, T.; Caldwell, J. W.; Kollman, P. A. *J. Am. Chem. Soc.* **1995**, *117*, 5179−5197.

(36) Jorgensen, W. L.; Chandrasekhar, J.; Madura, J. D. *J. Chem. Phys.* **1983**, *79*, 926−936.

(37) Chang, T.-M.; Dang, L. X.; Peterson, K. A. *J. Phys. Chem. B* **1997**, *101*, 3413−3419.

(38) Beudaert, P. Thesis, Université Louis Pasteur de Strasbourg, 1998.

(39) Lauterbach, M.; Engler, E.; Muzet, N.; Troxler, L.; Wipff, G. *J. Phys. Chem. B* **1998**, *102*, 225−256.

(40) Choi, K.; Tedder, D. W. *Spectrochim. Acta A* **1995**, *51*, 2301−2305.

(41) Nichimura, S.; Ke, C. H.; Li, N. C. *J. Am. Chem. Soc.* **1968**, *90*, 234−237.

(42) Naganawa, H.; Tachimori, S. *Anal. Sci.* **1994**, *10*, 309−314.

(43) Naganawa, H.; Tachimori, S. *Bull. Chem. Soc. Jpn.* **1997**, *70*, 809−819.

(44) Tedder, D. W. In *Science and Technology of TBP. Extraction of water and acids*; Schulz, W. W., Navratil, J. D., Kertes, A. S., Eds.; Boca Raton, FL, 1991; pp 35−122.

(45) Bullock, E.; Tuck, D. G. *Trans. Faraday Soc.* **1963**, *59*, 1293.

(46) Nishimura, S.; Ke, C. H.; Li, N. C. *J. Phys. Chem.* **1968**, *72*, 1297.

(47) Petkovic, D. M. *J. Inorg. Nucl. Chem.* **1968**, *30*, 603−609.

(48) Marcus, Y. *Chem. Rev.* **1963**, *63*, 139.

(49) Sheka, Z. A.; Kriss, E. E. *Zh. Neorg. Khim.* **1959**, *4*, 2505.

(50) Schaarschmidt, K.; Seifert, H.; Mende, G. *Z. Phys. Chem. (Leipzig)* **1967**, *235*, 22.

(51) Sergievskii, V. V.; Yaskin, V. V.; Evdokimova, L. V.; Yagodin, G. A.; Laskorin, B. N. *Radiokhimiya* **1981**, *23*, 49−51.
(52) Chaudry, M. A.; Ahmad, I. *J. Radioanal. Nucl. Chem.* **1991**, *148*, 15−26.
(53) Baaden, M.; Berny, F.; Wipff, G. *J. Mol. Liq.* **2001**, *90*, 3−12.
(54) Berny, F. Université Louis Pasteur, Strasbourg, 2000.
(55) This fully ionic acidic system with 30 neutral TBPs was also simulated with another initial state, starting from the end of the "standard" trajectory with HNO_3 (system ***C***), whose proton was transferred to the nearest water molecule, to form the H_3O^+ and NO_3^- ions.[66] Thus, initially, the ionic species were more randomized than in the ***D*** simulation. After 1 ns, this led to similar statitics and features as simulation ***D***, indicating that sampling in both cases is satisfactory. This is why we did not perform "demixing simulations" on system ***D***. The major difference comes from some acid species which remained trapped in chloroform because they were initially too far from the interface (i.e. beyond the cutoff distance) to "see" and interact with water molecules.
(56) Rao, P. R. V.; Kolarik, Z. *Solvent Extr. Ion Exch.* **1996**, *14*, 955−993.
(57) Miyake, C.; Hirose, M.; Yoshimura, T.; Ikeda, M.; Imoto, S.; Sano, M. *J. Nucl. Sci. Techn.* **1990**, *27*, 157−166.
(58) Sagert, N. H.; Quinn, M. J. *J. Colloid Interface Sci.* **1987**, *115*, 283−285.
(59) Erlinger, C.; Gazeau, D.; Zemb, T.; Madic, C.; Lefrançois, L.; Hebrant, M.; Tondre, C. *Solvent Extr. Ion Exch.* **1998**, *16*, 707−738.
(60) Stoyanov, E. *J. Chem. Soc., Faraday Trans.* **1998**, *94*, 2803−2812.
(61) Osseo-Asare, K. *Adv. Colloid Interface Sci.* **1991**, *37*, 123−173.
(62) Jacob, J.; Anisimov, M. A.; Sengers, J. V.; Oleinikova, A.; Kumar, A. *Phys. Chem. Chem. Phys.* **2001**, *3*, 829−831.
(63) Schnitzer, C.; Baldelli, S.; Campbell, D. J.; Shultz, M. J. *J. Phys. Chem.* **1999**, *103*, 6383−6386.
(64) Schnitzer, C.; Baldelli, S.; Shultz, M. J. *J. Phys. Chem. B* **2000**, *104*, 585−590.
(65) Mandin, C.; Martinet, L.; Zemb, T.; Berthon, L.; Madic, C. *CEA − Commissariat à l'Energie Atomique − Saclay. CEA-R-5930 − ISSN 0429-3460*, 2000.
(66) Baaden, M. Thesis, Université Louis Pasteur Strasbourg, 2000.
(67) Troxler, L.; Baaden, M.; Wipff, G.; Böhmer, V. *Supramol. Chem.* **2000**, *12*, 27−51.
(68) Naganawa, H.; Suzuki, H.; Tachimori, S. *Phys. Chem. Chem. Phys.* **2000**, *270*, 3247−3253.
(69) (a) Hynes, J. T. *Nature* **1999**, *397*, 565−566; (b) Schmidt, R. G.; Brickmann, J. *Ber. Bunsen-Ges. Phys. Chem.* **1997**, 1816−1827; (c) Laaksonen, K. E.; Klein, M. L. *J. Phys. Chem. A* **1997**, *101*, 98−102; (d) Ando, K.; Hynes, J. T. *J. Phys. Chem. B* **1997**, *101*, 10464−10478; (e) Ando, K.; Hynes, J. T. *J. Phys. Chem. A* **1999**, *103*, 10398−10408; (f) Mei, H. S.; Tuckerman, M. E.; Sagnella, D. E.; Klein, M. L. *J. Phys. Chem. B* **1998**, *102*, 10446−10458; (g) Sato, H.; Hirata, F. *J. Phys. Chem. B* **1999**, *103*, 6596−6604; (h) Billeter, S. R.; van Gunsteren, W. F. *J. Phys. Chem. A* **2000**, *104*, 3276−3286; (i) Berendsen, H. J. C.; Mavri, J. In *Theoretical Treatments of Hydrogen Bonding*; John Wiley & Sons: New York, 1997; pp 119−141.
(70) (a) Gao, J.; Li, N.; Freindorf, M. *J. Am. Chem. Soc.* **1996**, *118*, 4912−4913; (b) Tuckerman, M. E.; Laasonen, K.; Sprik, M.; Parrinello, M. *J. Chem. Phys.* **1995**, *103*, 150; (c) Laasonen, K.; Sprik, M.; Parrinello, M. *J. Chem. Phys.* **1993**, *99*, 9080; (d) Marx, D.; Tuckerman, M. E.; Hutter, J.; Parrinello, M. *Nature* **1999**, *397*, 601−604.
(71) Sullivan, D. M.; Bagchi, K.; Tuckerman, M. E.; Klein, M. L. *J. Phys. Chem. A* **1999**, *103*, 8678−8683.
(72) For instance, a recent simulation of nitric acid (no TBP) at the interface with 50% neutral (HNO_3) and 50% charged (NO_3^- H_3O^+) species shows that the neutral form is highly surface active, and attracts NO_3^- and H_3O^+ ions on the aqueous side of the interface via hydrogen bonding. (Berny, F. Thesis. Université Louis Pasteur, Strasbourg, 2000).
(73) Lauterbach, M.; Wipff, G. In *Physical Supramolecular Chemistry*; Echegoyen, L., Kaifer, A., Eds.; Kluwer Academic Publishers: Dordrecht, 199; pp 65−102.
(74) Chang, T. M.; Dang, L. X. *J. Chem. Phys.* **1996**, *104*, 6772−6783.
(75) Spohr, E.; Heinzinger, K. *Electrochim. Acta* **1988**, *33*, 1211−1222.
(76) Hautman, J.; Klein, M. L. *Mol. Phys.* **1992**, *75*, 379−395.
(77) Girault, H. H.; Schiffrin, D. J. In *Electroanalytical Chemistry*; Bard, A. J., Ed.; Dekker: New York, 1989; pp 1−141 and references therein.
(78) Koryta, J. In *Ion-Transfer Kinetics*; Sandifer, J. R., Ed.; VCH: New York, 1995; p 1.
(79) Starks, C. M.; Liotta, C. L.; Halpern, M. *Phase Transfer Catalysis*; Starks, C. M., Ed.; Chapmann & Hall: New York, 1994.
(80) Kazarinov, V. E. *The Interface Structure and Electrochemical Processes at the Boundary Between Two Immiscible Liquids*; Kazarinov, V. E., Ed.; Springer-Verlag: Berlin, 1987.
(81) Volkov, A. G.; Deamer, D. W.; Tanelian, D. L.; Markin, V. S. *Liquid Interfaces in Chemistry and Biology*; John Wiley & Sons: New York, 1998.